

MINERALOGY AND GEOCHEMISTRY STUDY OF REE MINERALS IN HOST ROCKS IN IIC IRON DEPOSIT, BAFGH MINERAL AREA, CENTRAL IRAN

*ESTUDO DE MINERALOGIA E GEOQUÍMICA DE MINERAIS REE EM ROCHAS HOSPEDEIRAS
NO DEPÓSITO DE FERRO DA IIC, ÁREA MINERAL DE BAFGH, IRÃ CENTRAL*
*ESTUDIO DE MINERALOGÍA Y GEOQUÍMICA DE MINERALES REE EN ROCAS HOSPEDANTES
DE DEPÓSITOS DE HIERRO DE LA CII, ÁREA MINERAL DE BAFGH, IRÁN CENTRAL*

<https://doi.org/10.26895/geosaberes.v11i0.909>

MANSOUREH SHIRNAVAR D SHIRAZI ¹
MOHAMMAD LOTFI ^{2*}
NIMA NEZAFATI ³
ARASH GOURABJERPOUR ⁴

¹ Department of Earth Science, Science and Research Branch, Islamic Azad University, Tehran, Iran. CP:56718-13146, Tel.:(+98) 9171028002, shirazi645@yahoo.com, <http://orcid.org/0000-0001-9242-0341>

² Department of Earth Science, North Tehran Branch, Islamic Azad University, Tehran, Iran. CP: 52148-2531, Tel.: (+98) 9121308075, m_lotfi_1014@yahoo.com, <http://orcid.org/0000-0002-2668-4485>

*Corresponding author.

³ Department of Earth Science, Science and Research Branch, Islamic Azad University, Tehran, Iran. CP: 45691-3691, Tel.: (+98) 09128083577, nima.nezafati@gmail.com, <http://orcid.org/0000-0002-5806-343X>

⁴ Department of Natural Resources, Myianeh Branch, Islamic Azad University, Miyaneh, Iran. CP: 147789-3855, Tel.: (+98) 9122477628, a.gourabjieri@yahoo.com, <http://orcid.org/0000-0001-8737-0634>

Article History:

Received 01 October, 2019.

Accepted 10 December, 2019.

Published 08 January, 2020.

ABSTRACT

The IIC deposit area to the east of the Bafq region exposes rocks that comprise the part of the Central Iran continental terrane. The IIC deposit iron orebodies are magmatic-related hydrothermal deposits that, when considered collectively display a vertical zonation from high-temperature, magmatic ± hydrothermal deposits emplaced at moderate depths (~1–2 km) to magnetite-dominant IOCG deposits emplaced at an even shallower subvolcanic level. The shallowest parts of these systems include near-surface, iron oxide-only replacement deposits, surficial epithermal sediment-hosted replacement deposits, and synsedimentary (exhalative) ironstone deposits. Alteration associated with the IOCG mineralizing system within the host volcanic, plutonic, and sedimentary rocks dominantly produced potassic with lesser amounts of calcic- and sodic-rich mineral assemblages. Our data suggest that hydrothermal magmatic fluids contributed to formation of the primary sodic and calcic alterations. The aim of this study is to delineate and recognize the different iron mineralized zones, based on surface and subsurface study. However, the data do not discriminate between a magmatic-hydrothermal source fluids resolved from Fe-rich immiscible liquid or Fe-rich silicate magma. Iron ores, occurring as massive-type and vein-type bodies are chemically different. Minor pyrite occurs as a late phase in the iron ores. The REE patterns of the mineralized metasomatites show LREE enrichment and strong Eu negative anomalies. The strong negative Eu anomaly probably indicates near-surface fractionation of alkali rhyolites involving feldspars. Field observations, ore mineral and alteration assemblages, coupled with lithogeochemical data suggest that an evolving fluid from magmatic dominated to surficial brine-rich fluid has contributed to the formation of the IIC deposit.

Palavras-chave: Mineralogy. Geochemistry. REE. IIC Iron deposit. Bafgh. Iran.

RESUMO

A área de depósito da IIC a leste da região de Bafq expõe rochas que compõem a parte do terrano continental do Irã Central. Os corpos orbitais de ferro da IIC são depósitos hidrotérmicos relacionados à magmática que, quando considerados coletivamente exibem uma zonação vertical de depósitos magmáticos ± hidrotérmicos de alta temperatura, colocados em profundidades moderadas (~ 1–2 km) a depósitos de IOCG dominantes por magnetita, colocados em um nível uniforme nível subvulcânico mais raso. As partes mais rasas desses sistemas incluem depósitos de substituição próximos à superfície, apenas com óxido de ferro, depósitos de substituição hospedados em sedimentos epitérmicos superficiais e depósitos de pedras de ferro sesedimentares (exalativas). As alterações associadas ao sistema de mineralização IOCG nas rochas vulcânicas, plutônicas e sedimentares do hospedeiro produzem predominantemente potássico com quantidades menores de conjuntos minerais ricos em cálcio e sódico. Nossos dados sugerem que fluidos magmáticos hidrotérmicos contribuíram para a formação das principais alterações sódicas e cálcicas. O objetivo deste estudo é delinear e reconhecer as diferentes zonas mineralizadas de ferro, com base em estudos de superfície e subsuperfície. No entanto, os dados não discriminam entre fluidos de fonte hidrotérmica magmática resolvidos a partir de líquido imiscível rico em Fe ou magma de silicato rico em Fe. Os minérios de ferro, que ocorrem como corpos maciços e veios, são quimicamente diferentes. Pirita menor ocorre como uma fase tardia nos minérios de ferro. Os padrões REE dos metassomatitos mineralizados mostram enriquecimento de LREE e fortes anomalias negativas da Eu. A forte anomalia Eu negativa provavelmente indica fracionamento próximo à superfície de riolitos alcalinos envolvendo feldspatos. Observações de campo, minerais de minério e conjuntos de alterações, juntamente com dados litoquímicos, sugerem que um fluido em evolução de magmático dominado a fluido rico em salmoura surficial contribuiu para a formação do depósito da IIC.

Keywords: Mineralogia. Geoquímica. REE. Depósito de ferro da IIC. Bafgh. Irã.

RESUMEN

El área de depósito de la CII al este de la región de Bafq expone rocas que comprenden la parte del terreno continental del centro de Irán. Los depósitos de mineral de hierro del depósito de la CII son depósitos hidrotermales relacionados con la magmática que, cuando se consideran colectivamente, muestran una zonificación vertical desde depósitos magmáticos ± hidrotermales de alta temperatura emplazados a profundidades moderadas (~ 1–2 km) hasta depósitos de COI dominantes con magnetita emplazados de manera uniforme. nivel subvolcánico menos profundo. Las partes menos profundas de estos sistemas incluyen depósitos de reemplazo de óxido de hierro cerca de la superficie, depósitos de reemplazo alojados en sedimentos epitermales superficiales y depósitos de piedra de hierro sinedimentarios (espiratorios). La alteración asociada con el sistema de mineralización IOCG dentro de las rocas volcánicas, plutónicas y sedimentarias del huésped produjo predominantemente potásico con cantidades menores de ensambles minerales ricos en calcio y sodio. Nuestros datos sugieren que los fluidos magmáticos hidrotermales contribuyeron a la formación de las alteraciones sódicas y cálcicas primarias. El objetivo de este estudio es delinear y reconocer las diferentes zonas mineralizadas de hierro, en base al estudio de superficie y subsuelo. Sin embargo, los datos no discriminan entre una fuente magmática-hidrotermal fluidos resueltos a partir de líquido inmiscible rico en Fe o magma de silicato rico en Fe. Los minerales de hierro, que se presentan como cuerpos de tipo venoso y masivo, son químicamente diferentes. La pirita menor ocurre como una fase tardía en los minerales de hierro. Los patrones REE de las metasomatitas mineralizadas muestran enriquecimiento LREE y fuertes anomalías negativas de Eu. La fuerte anomalía negativa de Eu probablemente indica un fraccionamiento cercano a la superficie de riolitas alcalinas que involucran feldspatos. Las observaciones de campo, el mineral mineral y los ensambles de alteración, junto con los datos litogeoquímicos, sugieren que un fluido en evolución desde fluido magmático dominado a fluido rico en salmuera superficial ha contribuido a la formación del depósito IIC.

Palabras clave: Mineralogía. Geoquímica. REE. IIC Depósito de hierro. Bafgh. Irán.

INTRODUCTION

The iron oxide-Cu-REE (Au) class of deposits have become a prime exploration target in the past decades and even earlier (HITZMAN, 2000). A consequence of the diversity in IOCG deposits, and of the brief time span since the recognition of this deposit group, is the diverging opinions on their genesis and the necessity of classifying them. With the current inadequate state of knowledge, genetic classifications are untenable and descriptive ones necessarily oversimplified and somewhat arbitrary (CORRIVEAU, 2006). In recent years the debate over this family of deposits has been increasingly focused on whether the fluids responsible for these systems are dominantly magmatically derived (POLLARD et al., 1998; WYBORN, 1998; SKIRROW, 1999; PERRING et al., 2000) or wall-rock controlled (HAYNES et al., 1995;

BARTON AND JOHNSON, 1996). HITZMAN (1992) grouped magnetite-apatite (Kiruna-type) and iron oxide-Cu-Au deposits together genetically. While there does appear to be a genetic link between the magnetite-apatite deposits (Kiruna-type) and the iron oxide-Cu-Au deposits, evidence suggests that they form end members of a continuum (HITZMAN, 2000). The iron oxide-(Cu-Au) deposit style (IOCG) is consistently associated with rare earth element (REE) enrichment, and consequently it is an ideal venue to study hydrothermal REE behavior during and following the emplacement of REE-bearing minerals (HITZMAN et al., 1992; HITZMAN, 2000). They consist of massive to brecciated, high temperature, magnetite-fluorapatite-calc-silicate bodies that may transgress or be transitional to regional alteration aprons of albite-actinolite \pm K-feldspar \pm phyllic alteration. They show a common association with evolved felsic intrusions, although the nature of the relationship between intrusions and IOA (Iron Oxide-Apatite ores) deposits is an area of substantial argument (PARAK, 1975; HILDEBRAND, 1986; NYSTRÖM, HENRIQUEZ, 1994; FRIETSCH, PERDAHL, 1995; BARTON, JOHNSON, 1996, 2004; TRELOAR, COLLEY, 1996; BROMAN et al., 1999; HITZMAN, 2000; SILLITOE, BURROWS, 2002; WILLIAMS et al., 2005).

Hydrothermal alkali-metasomatism is quite common and occurs in a large variety of geological environments and periods, from Archean to Cenozoic (CUNEY et al., 2012). Although average U and REE contents of ore bodies associated with alkali-metasomatism are not as high as in other types of ore deposits, they represent a promising exploration target because the resources of such deposits are relatively large, and despite their worldwide occurrence, they represent a significant underexplored type of mineral systems (CUNEY et al., 2012). The metasomatic and hydrothermal processes that take place with aqueous solutions are the only endogenic processes in which the concentration of radioactive elements, and primarily uranium, reach industrial concentration (Titayeva, 1994). The iron deposits are commonly hosted by hydrothermally altered and metasomatized rocks, which are either interstratified with volcano-sedimentary sequences, or form large subvolcanic and volcanic units (DALIRAN, 2002) and shallow intermediate to felsic intrusions (RAMEZANI, TUCKER, 2003).

The REE are mobile in certain geochemical systems involving aqueous media, as evidenced by analytical data for many natural waters including fluid inclusions, and also by enhanced concentrations of REE in metasomatized rocks; however, the mobility is limited and has led to some usage of the REE as immobile for modeling particular processes, such as rock alteration (see HENDERSON, 1996). Humphris (1989) concluded that there is no simple relationship between the degree of mobility of the REE and rock type or metamorphic grade, and emphasized the (1) mineralogical and (2) fluid controls. However, whether considering a magmatic immiscibility, magmatic hydrothermal, or a circulating brine hydrothermal genetic model for iron oxide deposits, it is now revealed that apatite can be subject to significant post-depositional REE leaching (ROEDDER et al., 1987; HARLOV et al., 2002; HEIDARIAN et al., 2018).

This discussion about central Iran has been running for more than 110 years (FÖRSTER, JAFARZADEH, 1994). Systematic investigation of the iron ore resources of the Bafq district began in 1968 with exploration by the former NISCO (National Iranian Steel Corporation) assisted by Soviet geologists. The results of this work were compiled in a series of internal reports by NISCO between 1969 and 1980. Despite this extensive body of geological and exploration data, the fundamental questions regarding the genesis of the iron ores remains open (DALIRAN, 2002).

Our contribution describes the petrology and geochemistry (with emphasis on REE) of an IOCG deposit, IIC deposit, from the BMD (Bafq Metallogenic District), Central Iran. The main approaches in this study are: (1) to introduce the IIC deposit ore deposit; (2) interpret the geochemical and petrologic data on the IIC deposit; (3) discuss the source and evolution of the

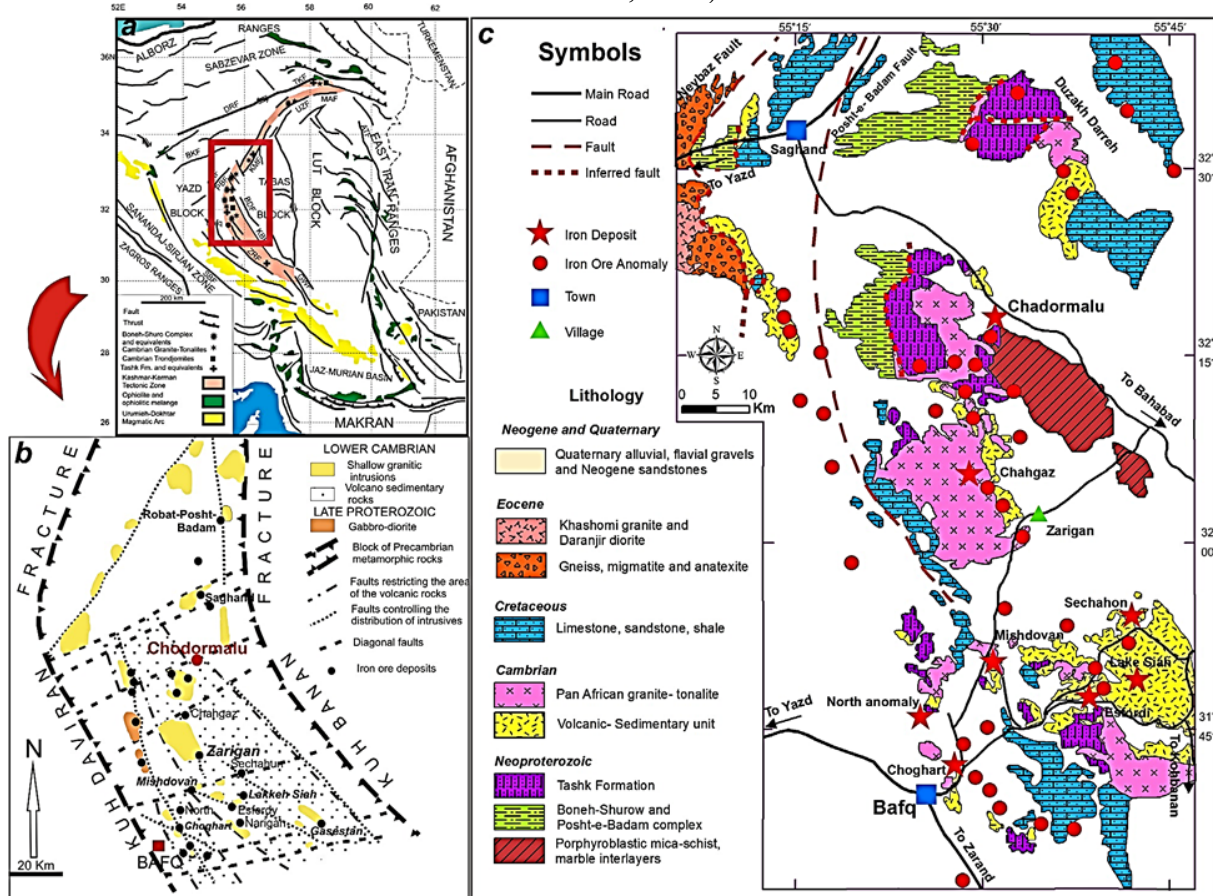
ore-forming fluid(s), conditions of ore formation and presentation a genetic model for the Fe mineralization in interpreting the geochemical and petrologic data on the IIC deposit.

GEOLOGICAL BACKGROUND

The BMD (Bafq Metallogenic District) is surrounded by fold-and-thrust belts, within the Alpine–Himalayan system of western Asia. The terrain is divided into three major crustal domains, from east to west: the Lut, Tabas, and the Yazd Blocks (ALAVI, 1991) (Figure 1A). The Bafq mining district lies in the Posht-e-Badam block (HAGHIPOUR, 1977; STÖCKLIN, 1971) or Kashmar-Kerman belt (RAMEZANI, TUCKER, 2003) in Central Iran (Figure 1A–C). The upper Proterozoic and Cambrian rocks are exposed in the arcuate Kashmar-Kerman structural zone, between the Kuh Daviran Fault and Kuh Banan faults (Figure 1B). The Early Cambrian tectonic regime has been interpreted as a rift (SAMANI, 1993; BARBARIN, 1999; DALIRAN, 2002). Ramezani and Tucker (2003) proposed that this feature was related to a broad-scale Andean margin on the edge of the Proto-Tethyan Gondwanaland supercontinent. Within the Cambrian sequence in the Kashmar-Kerman structural zone, deformation is largely limited to tilting and rotation of gently dipping fault blocks. The basement consists of medium- to high-grade metamorphic rocks of the Boneh Shurow (Amphibolite, Schist, Gneiss) and Posht-e-Badam (Gneiss, Micaschist, Marble, Amphibolite, Quartzite, and Metavolcanic) complexes intruded by intermediate intrusions (JAMI et al., 2007). The Neoproterozoic–Early Cambrian rocks consist of phyllites, slates, quartzites, and mafic volcanic rocks of the Tashk Formation (Jami et al., 2007), covered by a terrestrial to shallow marine sequence containing Ediacaran fauna (HAHN, PFLUG, 1980) and an Early Cambrian (530–528 Ma) bimodal volcanic unit (RAMEZANI, TUCKER, 2003). Rhyolite and dacite flows and tuffs associated with subordinate andesite, spilitic basalt, and rare nephelinitic to basanitic lava flows are the main intercalated volcanic rocks in the district. An important component of this (Bafq) is the Cambrian Volcano-sedimentary Unit (Desu series), composed of dolomite, limestone, sandstone, shale, and bimodal volcanic rocks (RAMEZANI AND TUCKER, 2003). The volcanic rocks predominantly occur as felsic domes of alkali rhyolite-rhyodacite (Mohseni, 2015) (Figure 1C). The close spatial and temporal association of the IOAs and the apatite-rich rocks with Early Cambrian felsic volcanic rocks suggest that mineralization and Early Cambrian magmatism were contemporaneous (DALIRAN, 2010). The sequence was intruded by small mafic to intermediate intrusive bodies and late doleritic dikes. All lithologies are locally subjected to syn- emplacement spilitization-keratophytic alteration (Jami et al., 2007). Despite valuable research data on BIFs, no distinguished cases are reported for the Ediacaran-type BIFs, except the few examples mentioned by Atapour and Aftabi (2012) and Pecoits (2010) yet considerable debate surrounds the exact genetic model of the Fe–P ores in the BMD, Iran. Förster and Jafarzadeh (1994) proposed a magmatic–carbonatitic–immiscible liquid and Daliran (1990, 2002) introduced the iron ore magma, magmatic–carbonatitic, Kiruna-type, hydrothermal–metasomatic, IOCG and IOA models of mineralization. Jami (2006) and Jami et al. (2007) suggested a primary oxide magmatic melt and also hydrothermal IOCG model for the Fe–P deposits of the BMD. Mohseni and Aftabi (2007) favored a glaciogenic Rapitan-type BIF, but Torab (2008) and Bonyadi et al. (2011) reappraised that the BMD deposits were of Cambrian felsic-related hydrothermal metasomatic IOCG–Kiruna ores. Mokhtari et al. (2013) reconsidered a magmatic immiscible liquid model of Förster and Jafarzadeh (1994) for the region, whereas Taghipour et al. (2013, 2015) suggested both magmatic and non-magmatic fluids, as well as skarn mineralization of Kiruna-type for the Choghart deposit. Narigan granite has been dated at 529 ± 16 Ma and 526 ± 2 Ma, respectively, using zircon U–Pb techniques (RAMAZANI, 1997). These granites are highly silicic, marginally peraluminous, and of trondhjemitic composition, with Na-rich plagioclase and low

K contents (RAMAZANI, 1997). Nevertheless, hypabyssal alkaline granites were probably emplaced in the back arc environment (cf. LENTZ, 1998).

Figure 1 - (a, b) Distribution of iron oxide–apatite sediments in Azarin Kashmar–Kerman volcanic belt (AMENDED after RAMEZANI, TALKER, 2003), (C) Revised geological map of Poshtebadam (AMENDED from HAGHIGHIPOUR 1977; NISCO, 1980; RAMEZANI, TUCKER, 2003).

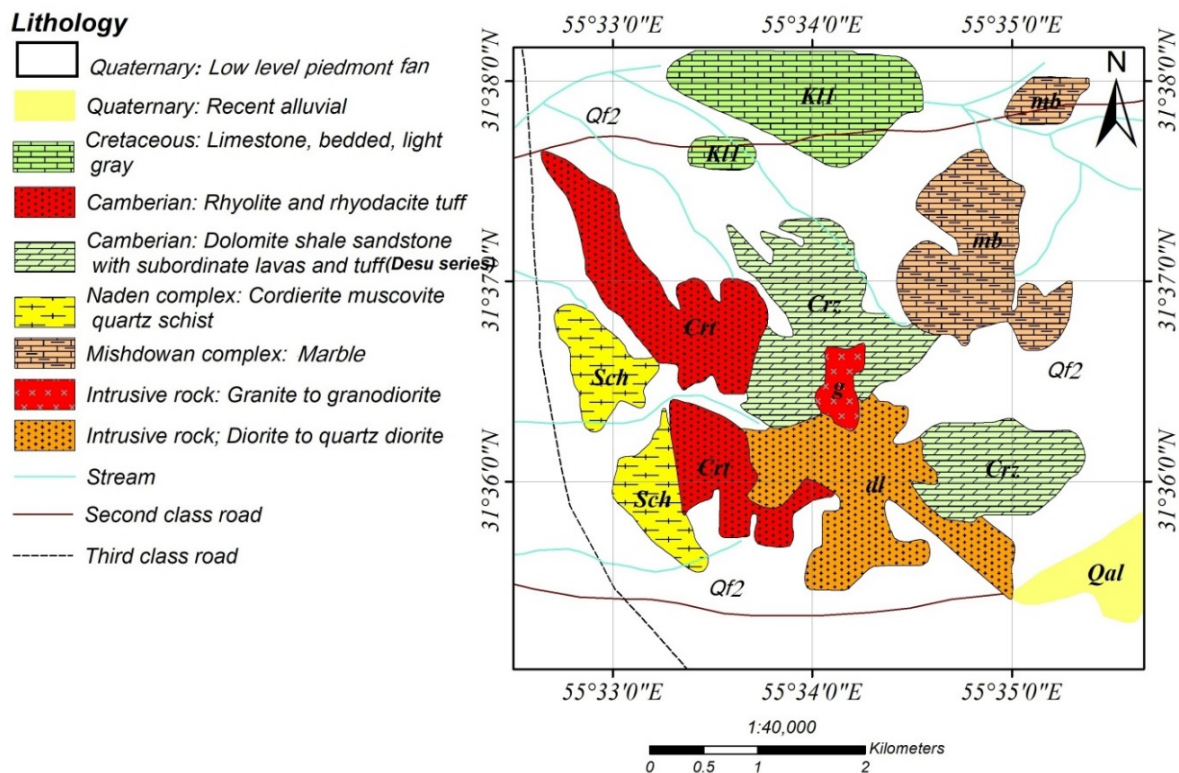


ORE DEPOSIT GEOLOGY

The Zaghia iron oxide deposit is located in the Bafq district. The IIC deposit is located east of Bafq city between $55^{\circ} 35' 38''$ at $55^{\circ} 31' 30''$ N and $31^{\circ} 37' 06''$ at $31^{\circ} 34' 40''$ E and part of Zaghia deposit. The main rock types in the vicinity of the deposit and the surrounding areas include felsic volcanic rocks, such as pinkish rhyolite and dacite locally associated, subvolcanic granites, as well as mafic to intermediate intrusive bodies and dikes, and schists (Figure 2). The zoned and strata-bound ore deposit has a prominent Fe-oxide-rich core and an overlying body of metasomatite and breccia that is rich in magnetite and hematite. Outcrops of metasomatic units exist in the northern and southern parts of the IIC deposit. Based on geological data (which include lithology and mineralogy) recorded from 30 drillcores and surface samples in the IIC deposit, major rock types in depth are metasomatite, conglomerate, limestone, tuff, magnetite, and hematite (SAGEGHI et al., 2012). The deposit area consists of a series of volcano-sedimentary units (Desu series), volcanic, plutonic, and metasomatic units. The IIC deposit the oldest rocks are mainly volcano-sedimentary rock (Desu series). The sedimentary rocks consist of dolomites, calcite, greywacke, and argillic-arenite sand-stone. The volcanic units contain are composed units of acidic volcanic rocks, such as rhyolite and dacite (rhyodacite) (Figure 3A).

Intruded into the CVSU (Cambrian Volcano-Sedimentary Unit), as well as into the Upper Precambrian metamorphic rocks, are plutonic bodies of mostly granitic composition (locally associated with diorite and gabbro-diorite dikes) (Figure 3A), which are quite common in Central Iran, of which the Narigan granites are located in the IIC deposit. Based mainly on their high sodium contents, Berberian and Berberian (1981) described these granitic intrusions as alkali granite (Figure 3B). The younger rocks (rhyolite and dacite) have been intruded in the older rock units (granite and granodiorite) unit (Figure 3A). Quaternary sediments overlapped the upper Cambrian units. All results show that the IIC host rock was completed before 544.6 ± 2.5 Ma (RAMEZANI AND TUCKER, 2003). Mohseni et al., (2007) suggest that the rocks of Bafq are keratophyres, jaspilites, diamictites, and dropstones together with the sedimentary source of fluorine-rich phosphorous. They introduce this deposit as a Rapitan-model type of iron–phosphorous mineralization rather than a minor model of IOCG for the Neoproterozoic–Early Paleozoic deposit. Sadeghi (2012) suggests that there is a strong relationship between mineralized zones and metasomatic units in the SE and central parts of the Zaghia deposit. The volcanic rocks predominantly occur as felsic domes of alkali rhyolite-rhyodacite. These are intruded by Cambrian granitoids and very late dabasic and lamprophyre dikes. The magnetite ores at the IIC deposit commonly occur within the felsic rocks such as rhyolitic and granitoids units.

Figure 2 - IIC deposit geological map (revised after Esfordi 1:100000 geological map).



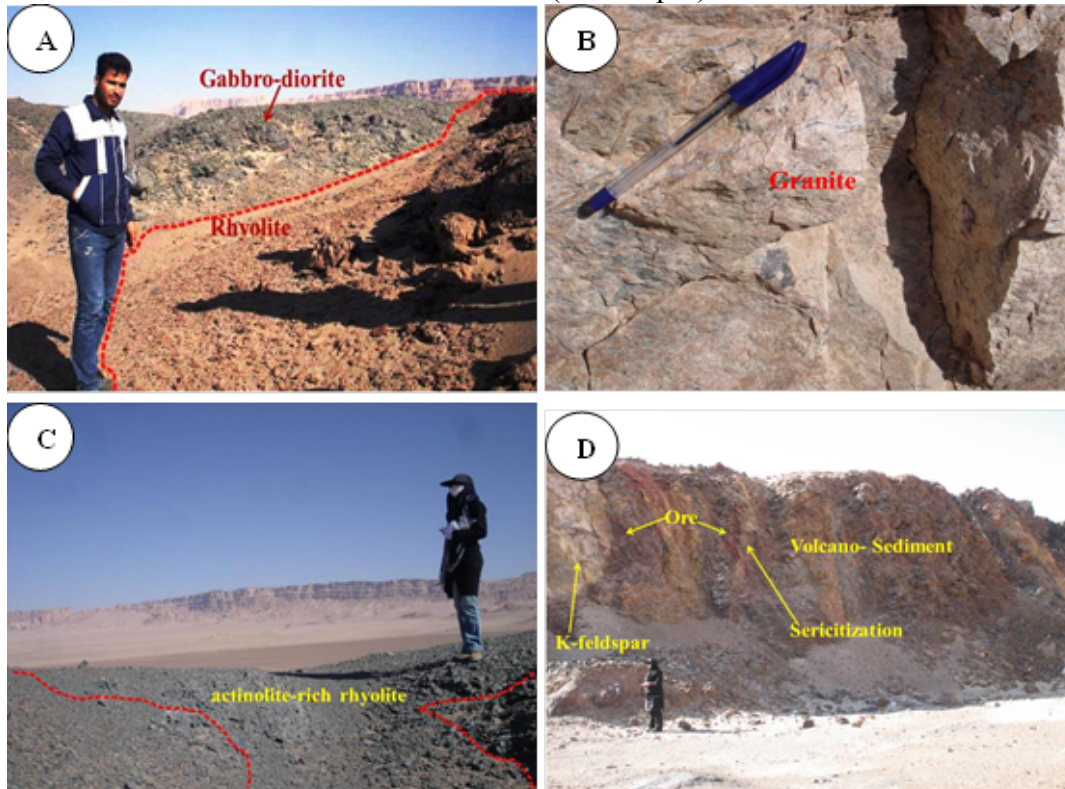
Source: Soheili and Mahdavi (1991).

ANALYTICAL METHODS

This research is done based on observation and sample collection in the field from the host rock. Detail analysis of petrography and geochemistry is performed on the samples. For

studying and exploration of this deposit, 30 samples of host rock (9 plutonic, 4 volcanic, 7 sediments, 10 metasomatic) for ICP (ICP-Mass Spectrometry) MS and XRF are collected and are analyzed in ZAR AZMA laboratory of minerals in Iran. Also 30 samples are chosen for petrographic and mineralogy (thin polish).

Figure 3 - Figures show base rock and IIC deposit. (A) Replacement of rhyodacite in gabbrodiorite (B) Granite with alteration of chlorite on its surface. (C) Actinolite alteration—changes of Na-Ca in base rock (D) Potassic alteration and the relation between deposit and volcanic unit (K-feldspar)



PETROLOGY

The volcano-sedimentary unit consists of dolomites, calcite, greywacke, and argillic-arenite sandstone. Magmatism is mainly felsic, composed of high-level rhyolite, subvolcanic dacite to rhyodacite. Mineralized rhyolites included quartz, albite, and sphene (titanite). The rhyolite unit has a granular texture (Figure 4A). Quartz is the most important mineral in the host rocks (plutonic and volcanic). Some of the quartz grains show undulatory extinction with deformational twinning. The youngest form of quartz occurs as veins that cut all of the geological units (Figure 4B). Hypogene replacement textures in the host rocks include replacement of chlorite, actinolite-tremolite, albite, sericite, and tourmaline in the structure of plagioclases, alkali feldspars, and mafic minerals (MOHSENI et al., 2015). Tremolite-actinolite form large and sometimes elongated crystals with magnetite in altered rhyolites (Figure 4C). Green color of actinolite is a reflection of the high iron content of the mineral and can imply that it is probably of ferroactinolite group. Similar actinolites have been reported to form at temperatures of 350-450°C in exhalative ore deposits (GALLEY, 2003). The intrusive rocks included diorite, monzogranite, granite, gabbro, and diabasic dikes.

Some intrusions of the granite and monzogranite suite have a fine-grained, but phaneritic, groundmass composed of mafic minerals (biotite) and felsic minerals, together with coarse- to

medium-grained quartz and feldspar phenocrysts. Intrusive rocks are small in size and in this deposit are fine-grained laminated rocks more or less altered to a quartz+feldspars+micas+tourmaline assemblage. Textural relations show that the chlorite replaces the structure of plagioclase and ferromagnesian minerals. Sericite after chlorite and actinolite is another abundant alteration mineral in the IIC deposit. Tourmaline show sometimes radiating clustered grains in thin sections. This mineral (tourmaline) is associated with sericite and probably formed by reaction of fluids rich in Fe-B with plagioclase, alkali feldspar, and chlorite. Actinolite and magnetite are developed within the albitized plagioclases and in groundmass (HEIDARIAN et al., 2017). The host rocks may have locally (in the minerals) undergone Fe-metasomatism, which occurred subsequent to the multistage alteration of the host rock, resulting in the growth of magnetite grains on the alteration quartz (late stage) and other alteration minerals (SABET, 2015). Amphibole metasomatism rocks contain euhedral to subhedral amphibole crystals. These amphiboles, based on optical properties and refractive indexes, are from tremolite - actinolite series (Shelly, 1993). Most amphiboles have been altered to secondary minerals, such as chlorite, calcite, and opaque minerals. Amphiboles are often associated with metasomatic albites. The actinolite-rich metasomatites comprise the main host rock of the IIC deposit (Figure 4C). These rocks are the product of intense actinolitization that replaced most minerals in the pre-alteration protolith. Actinolite would have a prominent role in the uptake of mobilized REE (particularly the HREE) and producing the bulk-rock REE patterns with flat HREE portions (Figure 6B), which is consistent with the compatibility of REE (particularly the HREE) in the amphibole structure (e.g., ROLLINSON, 1993). Albite metasomatism rocks contain plagioclase crystals with a microgranular texture. Plagioclase crystals are often subhedral to euhedral and most of them are albite and albite-pericline twinning. These minerals are mainly altered to clay minerals, chlorite, and sericite (Figure 4C). The term uralitization is generally accepted to describe an alteration of either an ortho or a clinopyroxene to amphibole so that the original crystal form of the pyroxene is preserved or still discernible.

The first phase of alteration indicates the introduction of iron and titanium into the pyroxene as small opaque grains, the pyroxene remaining otherwise unaltered. During the second phase small flakes of colourless actinolitic amphibole start to appear within the pyroxene; they increase in number and volume and at the end of this phase, they fill the entire space previously occupied by former pyroxene crystals. Chemically, this means that Fe, Ti, Al, K, and Na are introduced to the altering crystal from outside and Ca is transported from the mineral grain. After the colourless amphibole has filled the entire space of the former pyroxene crystals, tremolite-actinolite (uralitization phenomenon) begins to form at the outer edges of the grains. The green amphibole extends beyond the pseudomorph of the former pyroxene crystal boundaries (Figure 4D) (PILSPANEN et al., 1977).

LITHOGEOCHEMISTRY OF HOST ROCKS

Whole rock major- and trace-element compositions of least-altered rocks distal to the ore bodies are used for geochemical classification. The composition of the host rocks are presented in (Table 1), based on the lithogeochemical analysis (ICP-MS, XRF) in the IIC deposit. The magmatic rock classification is carried out for the IIC iron ore host rock (volcanic and plutonic) with (COX et al., 1979) model that indicate gabbro and granite types for plutonic and rhyolite and dacite for volcanic rocks (Figure 5A, B). The intermediate and felsic-composition suites are predominantly metaluminous, whereas the granite suite displays transitions to weakly metaluminous to peraluminous compositions. Chappell et al., (1974) recognized this compositional distinction in drawing their boundary between the I- and S-type granites, with a

limiting value for the Aluminium Saturation Index of 1.1, or 1% normative corundum. Chappell et al., (1992) pointed out that the most mafic compositions, which are closest to the source rocks in composition, there is no overlap between the I- and S-types. Shand (1943) placed the I-type granites in the metaluminous field (of Irvine and Baragar, 1971) and also extended the S-type granites into the metaluminous field (Figure 5C). To distinguish between calc-alkaline and tholeiitic suites, the samples were plotted on an AFM diagram that shows the samples mostly plot along the boundary between calc-alkaline and tholeiitic fields (Day et al., 2016) (Figure 5D). The intermediate and felsic compositions in the rock suite are relatively enriched in large ion lithophile elements (LILEs) and depleted in Ba, Nb, and Ti (Figure 6A). Nb and Y have concentrations typical of arc/syn collisional and within plate granites (Henderson, 1989). The negative Nb anomalies in the IIC deposit are consistent with concentrations of arc/syn collisional and within plate granites. P increases in abundance with fractionation of crystals from the more strongly peraluminous S-type felsic melts, whereas it decreases in abundance in the analogous, but weakly peraluminous, I-type melts (CHAPPELL et al., 1992). P decreases in the IIC deposit; it seems that P is entirely apatite (Figure 4E). Apatite's occur as disseminated euhedral grains and grain aggregates in the host rock.

Figure 4 - Photomicrographs of iron ore host rock in IIC deposit. (A) Carlsbad twinning in feldspars intersertal texture (CPL), brown sphene and epidote (CPL). (B) Filling with calcite and quartz veinlets (CPL). (C) Plagioclase crystallites altered to sericite (CPL). (D) Uralitization phenomenon from pyroxene (CPL). (E) Apatite needles developed on K-feldspar (PPL).

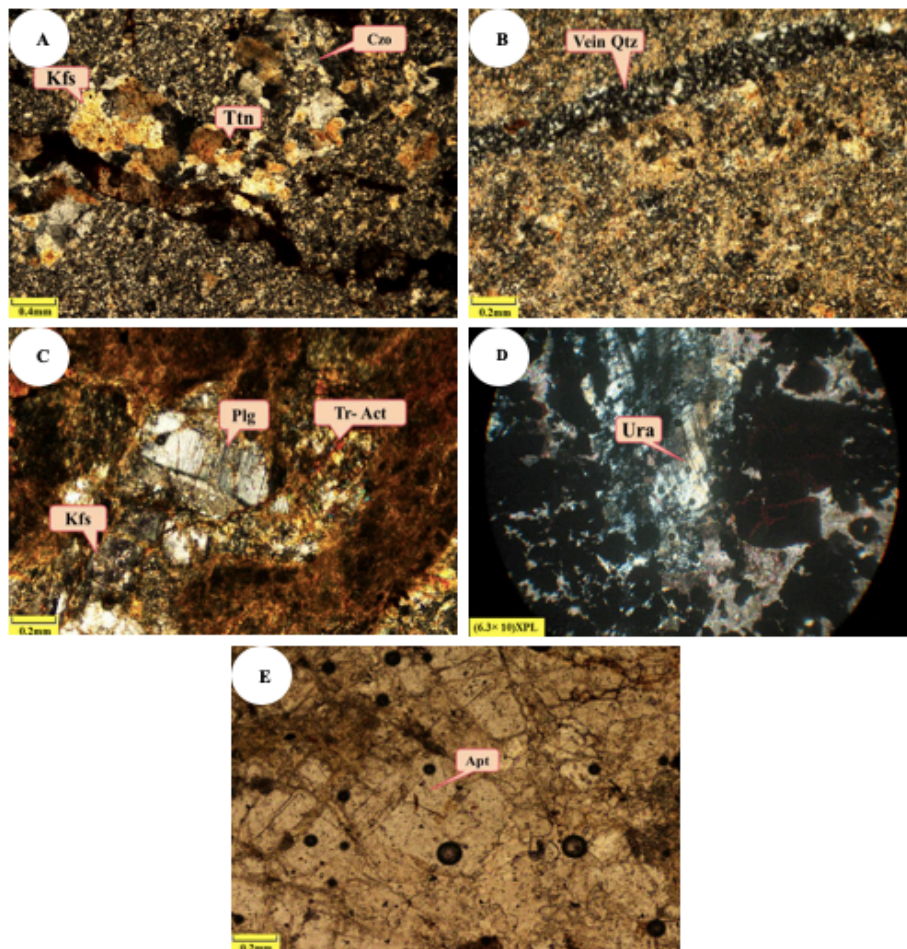
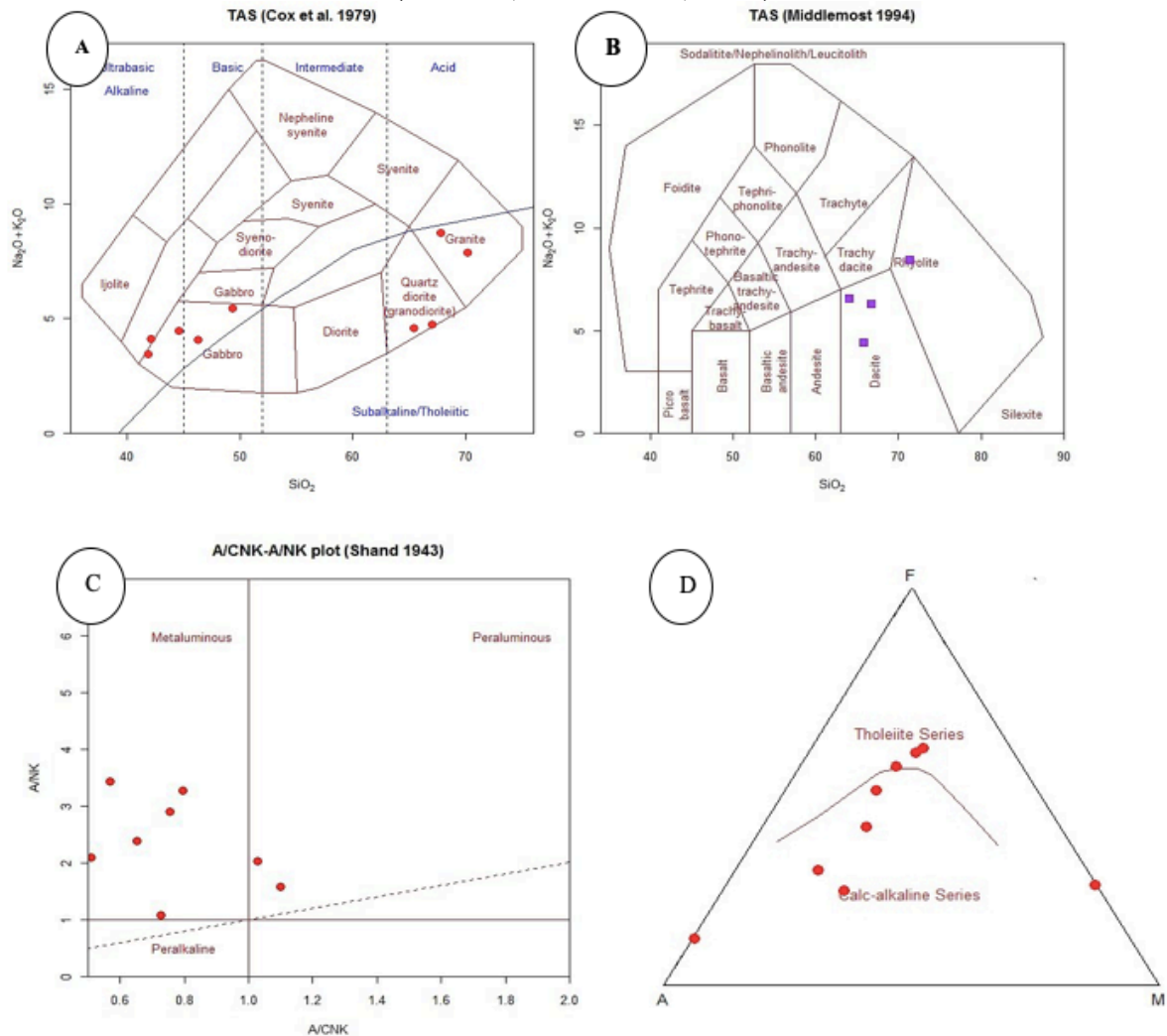


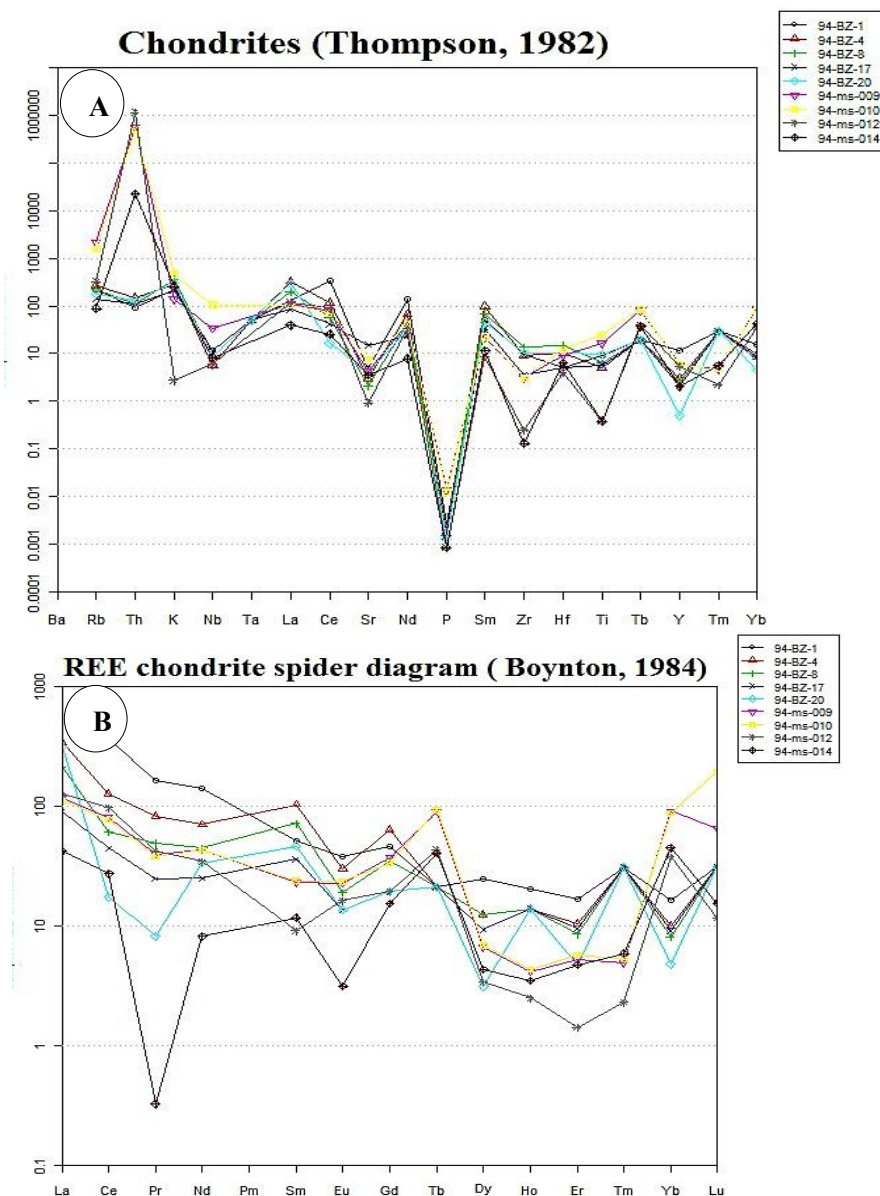
Figure 5 - Geochemical variation diagrams for plutonic and volcanic rocks from IIC deposit. (A) Classification of plutonic rocks based on (COX et al., 1979) model. (B) Classification of volcanic rocks based on the Middlemost (1998) model. (C) ACNK diagram for Al-saturation in granitoid rocks (SHAND, 1943). (D) AFM ($\text{Na}_2\text{O}+\text{K}_2\text{O}$ vs $\text{FeO}t$ vs MgO) Discriminant diagram between calc-alkaline and tholeiitic series of plutonic rocks of the IIC deposit (IRVINE, BARAGAR, 1971).



The chondrite-normalized rare earth element (REE) patterns show that host rocks exhibit notable enrichments in light REEs relative to heavy REEs, which is consistent with the dominant felsic and alkaline nature of the magmas in IIC deposit (cf. BARTON AND JOHNSON, 1996; GROVES et al., 2010). The REE concentrations have consistently elevated light REE (LREE) abundances with modest negative Pr anomalies (Figure 6B). While in magmatic liquids, middle rare earth elements (MREE) are more compatible in amphiboles than HREE (e.g., ROLLINSON, 1993), and the systematics of REE partitioning between fluid and mineral phases in relevant geological conditions to this study are not yet well-established. It can be postulated that the interaction of a fluid with a high HREE/LREE fractionation with the actinolite-rich host rocks could produce the HREE-elevated chondrite-normalized patterns of the host rock samples (SABET, 2015). These abundance differences have two origins. One simply relates a dilution by different amounts of volatile components, and the other represents

a nebula-wide fractionation of refractory elements (WHITNEY et al., 1998). The chondrite-normalized displays variably fractionated REE along with negative Eu anomalies. The REE concentrations have consistently elevated light REE (LREE) abundances with modest negative Eu anomalies. In addition, this group displays higher total REE abundances and a less pronounced negative Eu anomaly relative to those of the plutonic units. The host rocks show enriched LREE abundances and a negative Eu anomaly associated with IOCG deposits (Figure 6B) and presumably share a similar petrogenetic origin.

Figure 6 - (A) Chondrite-normalized spider diagram (THOMPSON, 1982). (B) REE chondrite-normalized spider diagram (BOYNTON,1984).



The oxidation state of Eu is dependent upon temperature, fO_2 , pH, and presence of complexing anions. The altered host rocks, especially the albitized rocks with higher albite abundances (up to 40%) have lower Eu contents and show negative Eu anomalies; this seems to be due to albitization of plagioclase under high oxygen fugacities (COX et al., 2013; Klinkhammer et al., 1994). Hydrothermal fluids without positive Eu anomaly have been

interpreted to be the result of extensive seawater contribution or mixing with detrital continental inputs (DOUVILLE et al., 1999; MARCHIG et al., 1982). If Eu was present largely as Eu^{3+} , only prior enrichment of the hydrothermal fluid in Eu can account for the positive anomaly (GOAD, 1996). Due to the compatibility of divalent Eu in plagioclase and K-feldspar structure, Eu anomalies are predominantly controlled by feldspars, particularly in felsic magmas (ROLLINSON, 1993). Additionally, Eu can exist in both the 2 and 3 oxidation states in magmatic systems, depending on the redox potential, which is a function of oxygen fugacity (HENDERSON, 1996). The negative Eu anomalies in the IIC deposit iron oxide melt as an indicator of the magmatic origin of the latter, and concluded that low oxygen fugacity promoted the immiscibility (HURAĪ et al., 1998). Mineralizing fluids equilibrated with the proposed Fe-P melts would have produced the negative Eu anomalies in the IIC deposit host rock. However, the plutonic samples (actinolite-rich) have relatively high REE contents and greater negative Eu anomalies than the feldspar-rich sample. The partitioning of Eu between fluid and solid phases in a hydrothermal system depends on its valency state which, in turn, strongly temperature-dependent at any is given oxygen fugacity (HENDERSON, 1996).

Table 1 - Major- and selected trace-element compositions of plutonic host rocks (all concentrations in ppm with the major oxides and Fe in wt.%).

Sample	94-BZ-1	94-BZ-4	94-BZ-	94-BZ-	94-BZ-	94-ms-	94-ms-	94-ms-	94-ms-
Elements									
SiO ₂ %	41.90	46.28	49.31	42.14	65.36	44.60	67.76	70.12	67.00
Fe%	15.62	7.06	7.32	11.05	3.22	15.70	15.65	1.16	1.40
Na ₂ O%	0.21	0.11	0.15	1.05	0.15	2.49	2.04	7.84	1.04
K ₂ O%	3.24	3.95	5.30	3.06	4.43	1.99	6.71	0.04	3.69
TiO ₂ %	0.92	0.51	0.65	0.60	1.00	1.69	2.56	0.04	0.04
P ₂ O ₅ %	0.12	0.08	0.07	0.07	0.06	0.63	0.58	0.04	0.04
Rb	79	92	80	49	63	761	544	114	31
Th	3.9	6.2	4.7	4.6	5.6	22502	20455	46631	927
U	25.1	25.4	3.6	2.7	1.4	17.0	7.0	46	25
Nb	4	2	3	4	3	12	37	2	3
Pb	43	13	11	19	15	0.38	0.38	0.38	0.38
Sr	56	35	25	177	46	50	87	11	42
Zr	67	62	92	25	71	21.8	21.1	1.7	0.9
La	145	105	65	28	97	36	34	39	13
Ce	291	102	49	36	14	65	62	78	22
Pr	20	10	6	3	1	4.87	4.65	5.16	0.04
Nd	85	42	27	15	20	26	25.9	20.7	4.9
Sm	10	20	14	7	9	4.51	4.64	1.78	2.29
Eu	2.8	2.2	1.4	1	1	1.68	1.72	1.2	0.23
Gd	12	16.4	9	5	5	9.66	8.7	5.03	3.99
Ga	15	8	8	10	4	0.68	0.7	0.25	0.17
Tb	1	1	1	1	1	4.27	4.39	2.06	1.91
Dv	8	4	4	3	1	2.15	2.22	1.1	1.39
Yb	3.4	2.1	1.7	1.9	1	18.9	18.3	7.9	9.3
Lu	1	1	1	1	1	2.1	6.2	0.375	0.5
Y	22.7	6.1	5	4.3	1	14.65	14.45	13.5	4.9
Cs	6.9	3.5	2.8	1.6	1.7	0.53	2.23	0.25	0.35

ALTERATION

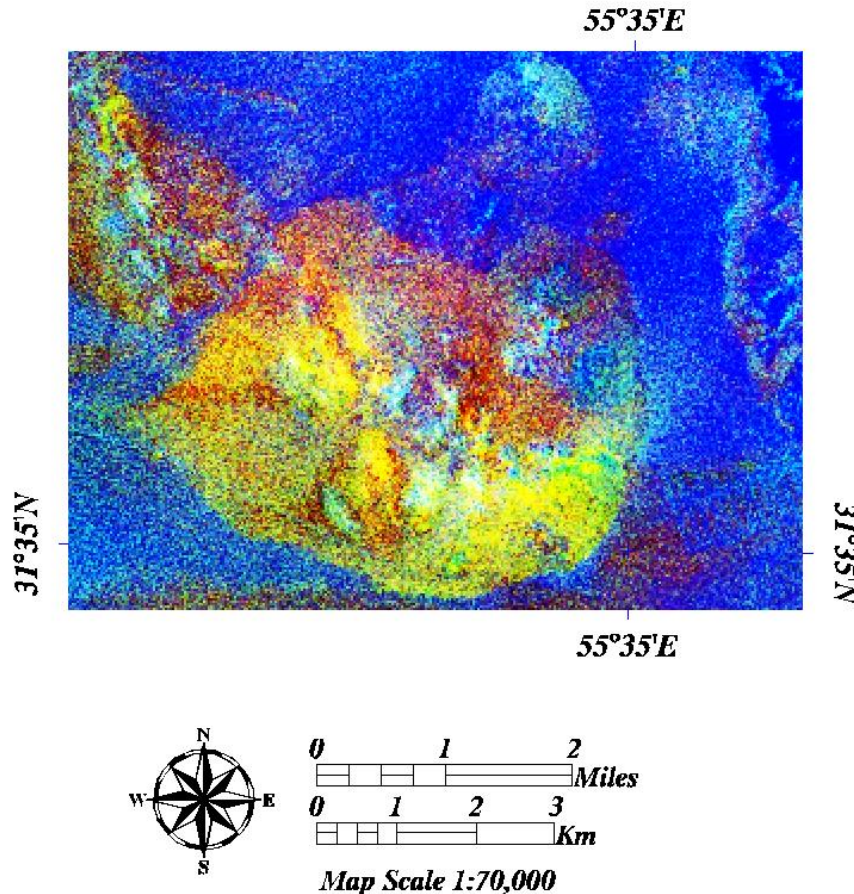
A striking characteristic of IOCG deposits is their alteration zones. Three main types are found: calcic-sodic, iron, and potassic alteration types. The calcic-sodic (Na-Ca) alteration zones are regional in scale (>1 km wide) and range from a strong albitization (\pm clinopyroxene,

titanite), with calc-silicate (clinopyroxene, amphibole, garnet)- alkali feldspar (K-feldspar, albite)± Fe-Cu sulphides, and various assemblages, including albite, actinolite, magnetite, apatite, and late epidote (CORRIVEAU, 2006). This early alteration is generally sodic (albite formation) or sodic-calcic (albite-amphibole), with temporally associated disseminated hematite (forming red-colored albite) and/or disseminated to veinlet magnetite. Calcic-iron-potassic alteration zones are well developed in deep parts of the IIC deposit showing, but are absent on surface. The sequence of facies begins with strong sodic-calcic alteration, dominated mainly by albite, except where deep red albitite forms and develops microcrystalline hematite and K-feldspar without significant increase in potassium and iron contents (MONTREUIL et al., 2015). Localized and pervasive magnetite-bearing and sodic alteration, potassic iron and hematite-bearing, potassic-iron alteration zones also enclose some of the Fe mineralized zones of the IIC deposit showings. The iron oxide mineralization mostly replaces metasedimentary rocks, but also forms veins and breccia filled near and within deformation zones (MUMIN et al., 1996; PORTER, 2010). The iron oxide-Cu-Au systems post-date the regional sodic and sodic-calcic alteration. The iron oxide-Cu-Au deposits and deposits may either directly overprint zones of earlier sodic or sodic-calcic alteration or show no particular spatial relationship to the earlier alteration event (HITZMAN, 2000).

Magnetite grains are developed on the earlier phases and on secondary actinolite grains. Sodic alteration, marked by replacive albitization, is widespread in the enclosing rocks. Calcic alteration dominated by actinolite occurs intensively and more proximal to the ore bodies. Potassic alteration is distinguished by development of K-feldspar replacing albite, as overgrowths on actinolite and sericitization of earlier minerals. Magnetite mineralization followed and partly replaced calcic and potassic alteration (HEIDARIAN et al., 2017). The alteration types in the IIC deposit are similar that alteration types above. According to field observations, the host rocks to the orebody is a highly altered actinolite-rich rhyolite. The host rock alteration is actinolitization (Figure 3C), which gives the host rocks a distinctive green appearance, however, sodic (albitization) and potassic (K-feldspar and sericitization) alteration types can also be observed and are related to the earlier stages of regional metasomatism in the IIC deposit (see also Daliran et al., 2007; Figure 3D). Quartz represents the late stage of hydrothermal alteration in the host rock (see also DALIRAN et al., 2007). Widespread sodic alteration, typically known by development of albite, has frequently been seen from Bafq iron district and IIC deposit (e.g., HAGHIPOUR, 1977; DALIRAN, 1990; JAMI, 2006; TORAB, 2008). The alteration has affected all rock types, including felsic volcanic and subvolcanic rocks and granites, and less commonly diorites, gabbros, rhyolite-rhyodacite, and schists. The sodic alteration resulted in the formation of fine- to coarse-grained albite, commonly displaying a chessboard texture (Figure 4C). Calcic alteration occurs as a proximal feature and dominates all other alteration products with proximity to the ore zones. The alteration is distinguished by actinolite replacing earlier mineral phases/rocks, including the Na-metasomatized albite-rich rocks. Fine-grained actinolite occurs in the groundmass and locally replacing or rimming albite crystals in volcanic and subvolcanic host rocks. Coarse actinolite crystals and crystal aggregates appear as needles or prismatic crystals in the groundmass and cutting earlier phenocrysts (Figure 4C). Calcic alteration is best developed in felsic volcanic and diorite host rocks. Potassic alteration, overprinting earlier sodic and calcic alteration assemblages, locally occurs in the host rocks. It is represented by K-feldspar mantling albite grains (Figure 4C), as well as disseminated K-feldspar grains in altered rocks (Figure 4A). Sericitic and silicic alteration types variably influenced all rock types and occur mainly in the upper parts of the system. Sericite occurs as replacing original magmatic minerals, as well as earlier alteration products. Silicic alteration occurs as newly formed fine-grained quartz in the groundmass (Figure 4B). The host rocks in IIC deposit are strongly altered by both early sodic (chessboard albite) and younger pervasive sodic-calcic alteration (amphibole-albite-magnetite-calcite-epidote-quartz-

titanite–allanite). Sodic-calcic (albitization) and calcic alteration developed in deep but there not seen on the surface. Potassic (K-feldspar and sericitization) alteration types can be observed and are related to the earlier stages of regional metasomatism in the IIC deposit (Figure 7).

Figure 7 - Band Ratio results for the potassic alteration (green, yellow and yellow- brown pixels), sericitization and chloritic alteration (bright blue pixels).

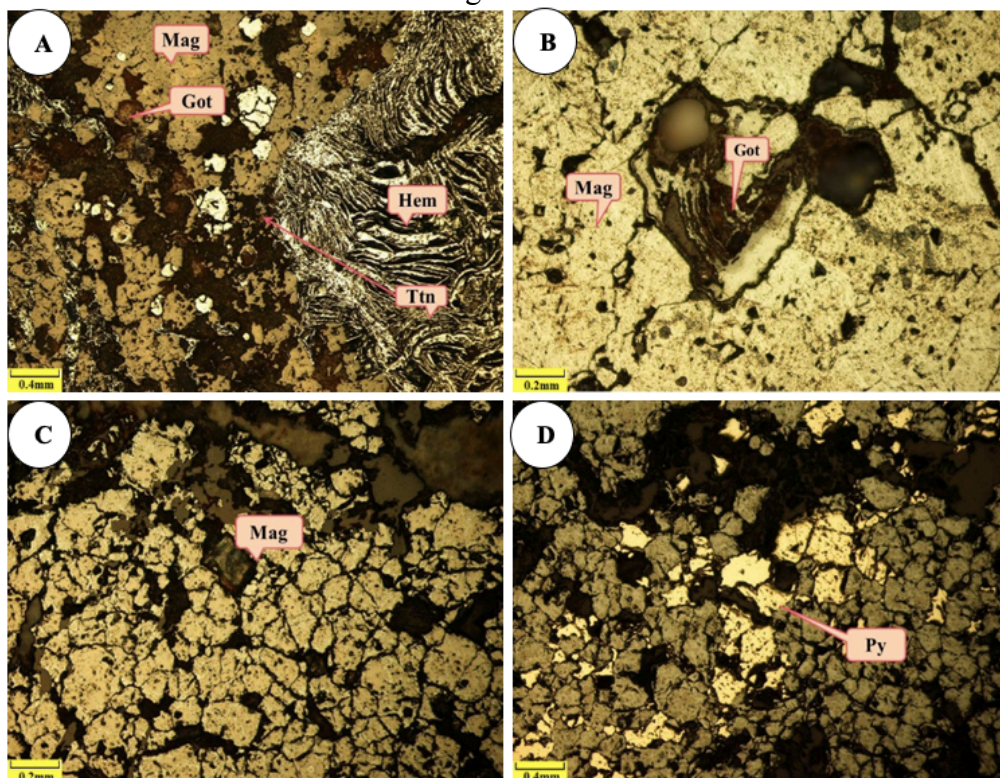


MINERALOGY OF ORE

The iron ore is included, such as hematite and magnetite particles, are observable in this area. Iron ore minerals are hematite, martite, specularite, limonite, goethite, magnetite, and pyrite. Ore-related hydrothermal alteration drastically changed the original features, producing complex partial to pervasive replacement textures, which are increasingly altered by proximity to ore bodies. The original features, however, can be distinguished with distance from the deposit (HEIDARIAN et al., 2017). The orebody consists of magnetite+hematite replacements of rhyolite. The open-space filling in the host rock includes actinolite+quartz. Sometimes, magnetites altered to hematite under the martitization event (Figure 8A). Quartz occurs as a late phase partially replacing actinolite grains implying a post-actinolite order in paragenesis. Sometimes weathering and supergene factors has caused hematite dissolution. So that progressive dissolution is causing the residual textures. Iron hydroxides, such as goethites and limonites, are formed from the weathering and supergene processes on previous ore. Sometimes these minerals are replaced partially in the margin and boundary fractures in primary ore minerals. Most of iron hydroxides have colloform texture that have replaced the form of crystals. Sometimes, these minerals can be observed as filamentous (Figure 8B). Magnetite is

common in igneous, metamorphic, and sedimentary rocks and can occur as or minerals in many types of deposits (DUPUIS et al., 2011). Magnetites are associated with apatite, calcite, quartz, and actinolite. Magnetite is a major ore mineral in this deposit with massive texture. The magnetite ore is typically fine grained. Magnetite is also found as small islands (relics) within pyrite. Secondary replacement reactions are common in magnetite as well as noted by Heidari et al. (2016). Magnetite occurring as overgrowths on actinolite and other phases formed due to continued infiltration by Fe-rich fluids. Quartz occurs in small vugs and veins in magnetite; the quartz occurs in the centers of the veins. Massive magnetites are indicative of a higher concentration of iron ions than silicic acid. Some of magnetite grains are extensive and they formed veins in the host rocks. This type of mineralization indicates support for the hydrothermal ore-forming processes (Figure 8C). In hematite-dominant samples, the hematite generally takes the form of specular aggregates of platy crystals up to 0.2 mm long with interstitial pyrite. In magnetite-dominant samples, the hematite can occur in irregularly shaped masses, as martite (pseudomorphs after magnetite). Pyrite is the most important sulphide phase within the iron ore in this deposit. Pyrite occurs as small euhedral to subhedral crystals. Pyrite crystals are developed as euhedral and well-formed crystals in fractures and cracks in the magnetite grains. This texture is indicative of the second generation of pyrite (Figure 8D). Sulfide mineralization in a classic IOCG deposits may be temporally associated with either calcic (amphibole, epidote, and/or carbonate) and/or potassic (biotite, potassium feldspar, or white mica in high level, hydrolytic systems) later alteration (DUPUIS et al., 2011). Iron ore mineralization has occurred in rhyolitic and granitoids.

Figure 8 - (A) Photomicrographs of the iron ore in IIC Iron deposit. (B) Replacement of magnetite with martite. (C) Goethite with colloform texture. (D) Pyrite between the magnetite grains.



DISCUSSION

The Bafgh district iron deposits have been extensively described and discussed; the genesis of the deposits, however, has long been a matter of debate. The IIC Iron oxide deposit is similar to hydrothermal Fe ore systems. The magnetite-apatite deposits (Kiruna-type) and the iron oxide-Cu-Au deposits form end members of a continuum. Generally, the magnetite-apatite deposits form prior to the copper-bearing deposits in a particular district (HITZMAN, 2000). The proposed evolution of the fluid cycle from sodic, during which extensive iron leaching took place, resulted in substantial Fe enrichment during calcic-iron alteration. The majority of the P-rich iron oxide deposits lack these later alteration stages.

Hydrothermal fluid temperature and changes in the chemical composition of the fluid, the late alteration stage occurred and veins of epidote±chlorite±muscovite were contemporaneously formed. By reducing the ratio of Na/Ca in the final fluid causes increasing K-H₂O; in fact hematite has deposited with muscovite. This process called hematite alteration by oxidation- acidic fluid (ROBB, 2005). Alteration that is associated with oxidizing fluids often results in the formation of minerals with a high Fe³⁺/Fe²⁺ ratio and, in particular, hematite with associated K-feldspar, sericite, chlorite, and epidote. Basically the presence of specularite in this stage is due to the function of an oxidant to relatively oxidize hydrothermal fluids. The specularite formed in the moderate to shallow, low temperature hydrothermal fluids or by reaction and mixing gases, which is rich in FeCl₃ with H₂O vapor (CORNELL et al., 2003). Also silicification is a part of this process. The hydrothermal models simply involve a mineralization process associated with hydrothermal alteration generated by hypersaline fluids to form magnetite deposits (DALIRAN, 2002; HITZMAN et al., 1992; JAMI et al., 2007; SILLITOE et al., 2002). Hematitization is evident along the fractures and joints. This indicates that hematitization increases more in the surface brittle zones. It seems that with approaching fluid surface and releasing the volatiles of such as CO₂, the forming alkali fluid has also become moderately acidic. Reduced temperature and pH causes enhanced liberation of REE in the host rocks (LOTTERMOSER, 1992). Magmatic models involving immiscibility between silicate and iron oxide-rich melts have widely been proposed for the genesis of Kiruna-type deposits (PHILPOTTS, 1967; FRIETSCH, 1978; NASLUND et al., 2000). All IOCG deposits contain enrichments of Fe, Cu, Au, and LREE. Individual deposits may contain trace to potentially economic levels of other metals (e.g., U and Ag at Olympic Dam, Zn at Candelaria). The diverse suite of trace metals in IOCG deposits is probably related both to the variable direct involvement of both ultrabasic to basic mantle-derived magmas (elements such as Ni and Co) and leaching of metals from large volumes of crustal material (HITZMAN et al., 2005).

In this study, field and mineralogical observations and other geochemical patterns have been used to construct a genetic model for the IIC deposit and associated hydrothermal alteration. The IIC deposit displays hydrothermal alteration products similar to those recognized at other iron oxide-Cu-Au deposits. Early sodic alteration was pervasive, due to infiltration of hydrothermal fluids along fractures and grain boundaries. Later, calcic and potassic alteration also was localized by shear zone development. Fluid flow related to these early alteration stages was controlled by permeability in large-scale regional shear and fault zones. Fluid sources and their evolution have been determined by several lines of evidence. Extensive Na-rich alteration in the IIC deposit host rocks require a highly saline fluid that cannot plausibly be generated from associated magmas (see Barton and Johnson, 1996). A generally consistent pattern of early regional sodic alteration (albite-hematite), similar to that reported from other iron oxide-Cu-Au deposits in the Bafq district was followed by calcic

alteration (represented by actinolite), and then potassic alteration and magnetite-(apatite) formation. An extensive alkali-rich alteration system of iron-rich sodic, calcic, and potassic types is consistent with evidence for an iron oxide-Cu-Au deposits. Sericitization and silicic alteration and carbonatization are other hydrothermal alteration types, which developed during or after mineralization. These lower temperature alteration assemblages are interpreted as shallow level alteration, in contrast to the sodic and calcic assemblages, and might be related to hydrolytic alteration occurring due to the post-mineralization episode(s) of fluid circulation at shallower depths. The IIC magnetite ore and its host rocks display relatively LREE-enriched patterns, which can reflect a felsic magmatic origin (cf. GROVES et al., 2010 and references therein; MARSCHIK et al., 2000; RAY, DICK, 2002; SILLITOE, 2003), or a host-rock control independent of magmatic processes (e.g., BARTON, JOHNSON, 1996, 2000, 2004). The IIC deposit REE concentrations have consistently elevated light REE (LREE) abundances with modest negative Eu anomalies. In addition, this group displays higher total REE abundances and a less pronounced negative Eu anomaly relative to those of the precambrian rhyolite and granites units. Primary magnetites from the massive ores formed from high temperature magmatic dominated hydrothermal fluids, whereas secondary varieties, which replaced primary ones, especially in the vein-type ore body, were developed in the presence of high salinity-low temperature evaporitic fluids.

Magnetite-rich deposits can be expected to form from such fractions at high temperatures in subsurface environment, and hematite-rich deposits at relatively lower temperatures in near surface and subaerial environments. For some of the hematite-rich stratabound deposits, there are differences of opinion as to whether hematite was deposited as primary iron oxide from hydrothermal solution, formed as a replacement of magnetite and other minerals, or was precipitated in a marine exhalative-sedimentary environment. Replacement may be due to the action of hydrothermal fluids, or of oxidized ground waters if a deposit was subjected to weathering processes.

CONCLUSION

The IIC deposit is one of the iron oxide deposits in the Bafgh district, hosted in the Precambrian-Cambrian igneous rocks, and represents several characteristics of IOCG deposits including:

- The sedimentary/volcanic successions, metamorphic rocks and magmatic intrusions exposed in the deposit IIC of the Central Iranian.
- At the IIC deposit multiple different alteration events occurred from sodic (and sodic-calcic to potassic, sericitic, and silicic in the deposit.
- Another evidence for high-temperature fluids at the IIC deposit includes the pervasive replacement of the rock by actinolite, which resulted in the formation of the actinolite-rich metasomatic host rocks.
- Whereas REE contents display a coherent variation fluids and important fractionation may occur during alteration. The rocks from the IIC deposit are LREE rich, and have negative Eu anomalies. Moreover, the Fe-melt has been mixed from it by liquid immiscibility, which separated from a silica-rich melt. Based on the REE geochemistry it is proposed that a potential source for metals would be late stage Fe melt differentiates of the Cambrian magmatism, which is consistent with the late Fe-metasomatism in the host rocks.
- Magnetite showing various primary and secondary textures formed during a prolonged history of ore Fe. Minor pyrite occurs as a late crack filling phase and overgrowth on magnetite.

•Lithogeochemical data are representative of calc-alkaline nature for magmatic rocks and reflect contribution and mixing of different magma sources in the evolution of the hydrothermal ore-forming fluids.

It can be concluded from the above evidence, that a mixed sourced fluid including magmatic hydrothermal and brine fluid was responsible for the formation of the IIC deposit. Given the results mentioned above, we suggest that the mineralogical and geochemical data are best interpreted in terms of a magmatic origin for the mineralization in the IIC deposit. However, it can be inferred that high temperature fluids differentiated from calc-alkaline granitoid magma would have ascended along faults and fractures, and after the proximity to the surface and the fluid/rock reaction, caused the metasomatism, hydrothermal alteration and mineralization. In this model, granitoid magma and diorite-quartz diorite rocks serve as the source and hosts for mineralization, respectively. Evidences suggest that the IIC deposit iron ore are similar to Iron oxide (Cu+Au+U+REE) ore deposits.

REFERENCES

ATAPOUR, H., AFTABI, A (2012). **Rapitan-type banded iron formation at Hormouz Island, Iran:** geological survey of Iran. The 30th Symposium, Programme with Abstracts (in Persian) With English Abstract.

ALAVI, M (1991). **Tectonic map of the Middle East (scale 1:5, 000, 000).** Geological Survey of Iran.

BARBARIN, B (1999). A review of the relationships between granitoid types, their origins and their geodynamic environments, **Lithos**, Volume 46, Issue 3, March 1999, Pages 605–626.

BERBERIAN, F., BERBERIAN, M.(1981). Tectono-plutonic episodes in Iran, In: GUPTA, H.K., and DELANY, F.M., editors, **Zagros-Hindu Kush-Himalaya geodynamic evolution:** American Geophysical Union Geodynamic Series, v. 3, p. 5-32.

BARTON, M.D., JOHNSON, D.A (2000). Alternative brine sources for Fe-oxide (Cu–Au) systems: Implications for hydrothermal alteration and metals. In: PORTER, T.M. (Ed.), **Hydrothermal Iron Oxide Copper-Gold and Related Deposits:** A Global Perspective. Australian Mineral Foundation, Glenside, SA, pp. 43–60.

BARTON, M.D., JOHNSON, D.A (2004). **Footprints of Fe oxide (-Cu- Au) systems:** University of Western Australia Special Publication, v. 33, p. 112-116.

BARTON, M. D. & JOHNSON, D. A (1996). Evaporitic source model for igneous-related Fe oxide-(REE-Cu-Au-U) mineralization. **Geology** 24, 259-262.

BONYADI, Z., DAVIDSON, G.J.,MEHRABI, B.,MEFFRE, S., GHAZBAN, F (2011). Significance of apatite REE depletion and monazite inclusions in the brecciated Se-Chahun iron oxide– apatite deposit, the Bafq district, Iran, insights from paragenesis and geochemistry . **Chem. Geol.** 281, 253–269.

BROMAN, C., NYSTRÖM, J.O., HENRÍQUEZ, F., ELFMAN, M (1999) . Fluid inclusions in magnetiteapatite ore from a cooling magmatic system at El Laco, Chile . **GFF** 121, 253–267.

CHAPPELL, B. W., WHITE, A. J. R (1992). I – and S –type granites in the Lachlan fold belt. **Royal Society of Edinburgh Transaction Earth Sciences**, Vol. 83, pp. 1-26.

CHAPPELL, B.J. WHITE, A.J.R (1974). Two contrasting granite types. **Pacific Geology**. Vol 8. pp.173-174.

CORNELL, R. M., SCHWERTMANN, U (2003). **The iron oxides**. 2nd. Wiley-VCH; 613 p.

CORRIVEAU, L., WILLIAMS, P.J., MUMIN, A.H (2010A). Alteration vectors to IOCG mineralization from uncharted terranes to deposits: **Geological Association of Canada Short Course Notes**, v. 20, p. 89–110.

CORRIVEAU, L (2006). Iron oxide copper-gold ($\pm\text{Ag}\pm\text{Nb}\pm\text{P}\pm\text{REE}\pm\text{U}$) Deposits: A Canadian perspective. **Natural Resources Canada**, Geological Survey of Canada.

COX, G.M., HALVERSON, G.M., MINARIK, W.G., LE, H.D.P., MACDONALD, F.A., BELLEFROID, E.J., STRAUSS, J.V (2013). Neoproterozoic iron formation: an evaluation of its temporal, environmental and tectonic significance. **Chem. Geol.** 362, 232–249.

COX, K.G., BELL, J.D., PANKHURST, R. J (1979). **The Interpretation of Igneous Rocks**. George Allen & Unwin.

CUNEY, M., EMETZ, A., MERCADIER, J., MYKCHAYLOV, V., SHUNKO, V., YUSLENKO, A (2012). Uranium deposits associated with Na-metasomatism from central Ukraine: a review of some of the major deposits and genetic constraints. **Ore Geol. Rev.** 44, 82–106.

DALIRAN, F., STOSCH, G., WILLIAMS, P., (2007). Multistage metasomatism and mineralization at hydrothermal Fe oxide-REE-apatite deposits and apatites of the Bafgh district, central-east Iran. In: Stanely C. J. eds. Digging Deeper, pp. 1501_1504. Proceedings 9th Biennial SGA Meeting Dublin, Ireland Ficher, R. P. 1950, Uranium Bearing Sandstone Deposits of the Colorado Plateau: **Economic Geology**, v. 45, p. 1-11.

DALIRAN, F (2002). Kiruna-type iron oxide–apatite ores and -apatites of the Bafq district, Iran, with an emphasis on the REE geochemistry of their apatites. **A Global perspective** 2 pp. 303–320.

DALIRAN, F (1990). **The magnetite–apatite deposit of Mishdovan, Eastcentral Iran, an alkaline rhyolite hosted-Kiruna type occurrence in the Bafq metalotect**. Mineralogic, Petrographic and Geochemical Study of the Ores and the Host Rocks Heidelberg Geowiss Abh 37 (248 pp).

DAY, WARREN C, SLACK, JOHN F., AYUSO, ROBERT A, SEEGER, CHERYL. M (2016). Regional Geologic and Petrologic Framework for Iron Oxide \pm Apatite \pm Rare Earth Element and Iron Oxide Copper-Gold Deposits of the Mesoproterozoic St. Francois Mountains Terrane, Southeast Missouri, USA, **Economic Geology**, v. 111, pp. 1825–1858.

DOUVILLE, E., BIENVENU, P., LUC, C.J., DONVAL, J.P., FOUQUET, Y., APPRIOU, P., GAMO, T (1999). Yttrium and rare earth elements in fluids from various deep-sea hydrothermal systems. **Geochim. Cosmochim. Acta** 63, 627–643.

DUPUIS, C., AND BEAUDOIN, G (2011). Discriminant diagrams for iron oxide trace element fingerprinting of mineral deposit types: **Mineralium Deposita**, v. 46, p. 319– 335.

FÖRSTER, H., JAFARZADEH, A (1994). The Bafq mining district in central Iran-a highly mineralized Infracambrian volcanic field. **Econ. Geol.** 89, 1697–1721.

FRIETSCH, R., (1978). On the magmatic origin of iron ores of the Kiruna type. **Economic Geology**, Vol. 73, pp. 478–485.

FRIETSCH, R., PERDAHL, J.A (1995). Rare earth elements in apatite and magnetite in Kirunatyp iron ores and some other iron ore types. **Ore Geol. Rev.** 9, 489–510.

GALLEY, A.G (2003). Composite synvolcanic intrusions associated with Precambrian VMS hydrothermal systems, **Mineralium Deposita** 38, 443-473.

GIFKINS, C.C.; HERRMANN, W.; LARGE, R.R (2005). **Altered Volcanic Rocks: A Guide to Description and Interpretation**; Centre for Ore Deposit Research, University of Tasmania: Hobart, Australia.

GOAD, R.E., MUMIN, A.H., AND MULLIGAN, D.L (1996). A report on the geology of the JBG1-7 claims, Marian River area, Mackenzie (south) district, Northwest Territories, Canada: **NWT Geoscience Office**, NORMIN Assessment Report 083776, 89 p.

GROVES, D.L., BIERLEIN, F.P., MEINERT, L.D., AND HITZMAN, M.W (2010). Iron oxide copper-gold (IOCG) deposits through Earth history: Implications for origin, lithospheric setting, and distinction from other epigenetic iron oxide deposits: **Economic Geology**, v. 105, p. 641–654.

HAGHIPOUR, A (1977). **Geological Map of the Biabanak-Bafq Area (scale 1:500, 000)**. Geological Survey of Iran.

HAHN, G., PFLUG, H. D (1980). Ein neuer Medusen-Fundausdem Jung prikambrium von Zentral-Iran: **Senckenbergiana Lethaea**, 60, 449-461 (with English abstract).

HARLOV, D.E., ANDERSSON, U.B., FÖRSTER, H.J., NYSTRÖM, J.O., DULSKI, P., BROMAN, C (2002). Apatite monazite relations in the Kiirunavaara magnetite-apatite ore. northern Sweden. **Chem. Geol.** 191, 47–72.

HAYNES, D. W., CROSS, K. C., BILLS, R. T., & REED, M. H (1995). Olympic Dam ore genesis: A fluid-mixing model. **Economic Geology** 90, 281-307.

HENDERSON, P (1989). Rare earth element geochemistry. **Elsevier**. p. 510.

HEIDARIAN, H.; ALIREZAEI, S.; LENTZ, D.R (2017). Chadormalu Kiruna-type magnetite-apatite deposit, Bafgh district, Iran: Insights into hydrothermal alteration and

petrogenesis from geochemical, fluid inclusion, and sulfur isotope data. **Ore Geology Review** 83, 43-62.

HEIDARIAN, H., LENTZ, D.R ALIREZAEI, S., MCFARLANE, C.R. M., PEIGHAMBARI, S (2018). **Multiple Stage Ore Formation in the Chadormalu Iron Deposit, Bafgh Metallogenic Province, Central Iran: Evidence from BSE Imaging and Apatite EPMA and LA-ICP-MS U-Pb Geochronology.** *Minerals* 2018, 8, 87.

HILDEBRAND, R.S (1986). Kiruna-type deposits: their origin and relationship to intermediate subvolcanic plutons in the Great Bear Magmatic Zone, northwest Canada. **Econ. Geol.** 81, 640–659.

HITZMAN, M.W. AND VALENTA, R.K (2005). Uranium in iron oxide- copper-gold (IOCG) systems: **Economic Geology**, v. 100, p. 1657-1661.

HITZMAN, M. W (2000). Iron oxide–Cu–Au deposits: what, where, when, and why? In: Porter TM (ed) Hydrothermal iron oxide– copper–gold and related deposits—a global perspective. **PGC Publishing**, Vol. 1. pp 9–25.

HITZMAN, M. W (1992). Olympic Dam type Fe-Cu-REE deposits - a preliminary model and an example from the Proterozoic of Yukon Territory, Canada [abs.]. **International Geol. Congress**, Abstracts, Kyoto, 3- 740.

HUMPHRIS, S.E (1989). The mobility of the rare earth elements in the crust. In: Henderson P (ed) Rare earth element geochemistry. **Elsevier Science Publishers B.V.**, Amsterdam, pp 317–342

HURAI, V., SIMON, K., WIECHERT, U., HOEFS, J., KONECNY, P., HURAIŇOVA, M., PIRONON, J., LIPKA, J (1998). Immiscible separation of metalliferous Fe/ Ti oxide melts from fractionating alkali basalt: P- T-fO₂ conditions and two-liquid elemental partitioning. **Contrib Mineral Petrol** 133:12–29.

IRVINE, T. N., AND BARAGAR, W. R. A (1971). A guide to the chemical classification of the common volcanic rocks. **Canadian Journal of Earth Sciences.**, Vol. 8, pp. 523–548.

JAMI, M., DUNLOP, A.C., COHEN, D.R (2007). Fluid inclusion and stable isotope study of the Esfordi apatite- magnetite deposit, **Central Iran.** **Econ. Geol.**, 102, 1111–1128.

JAMI, M (2006). **Geology, geochemistry and evolution of the Esfordi phosphate-iron deposit, Bafq area, Central Iran.** Unpublished PhD Thesis, The University of New South Wales, Australia.

KLINKHAMMER, G.P., ELDERFIELD, H., EDMOND, J.M., MITRA, A (1994). Geochemical implications of rare earth element patterns in hydrothermal fluids from midocean ridges. **Geochim. Cosmochim. Acta** 58, 5105–5113.

LENTZ, D.R (1998). Petrogenetic and geodynamic implications of extensional regimes in the Phanerozoic subduction zones and their relationship to VMS-forming systems. **Ore Geol. Rev.** 12, 289–327.

LOTTERMOSER, B.G (1992). Rare earth elements and hydrothermal ore formation processes. **Ore Geology Reviews.**, Vol. 7, Issue 1, pp 25- 41.

MARCHÍG, V.; GUNDLACH, H.; MÖLLER, P.; SCHLEY, F (1982). Some geochemical indicators for discrimination between diagenetic and hydrothermal metalliferous sediment. **Mar. Geol.** 50, 241–256.

MARSCHÍK, R.; LEVEILLE, R.A.; MARTÍN, W (2000). La Candelaria and the Punta del Cobre district, Chile: early Cretaceous iron-oxide Cu– Au(–Zn–Ag) mineralization. In: PORTER, T.M. (Ed.), **Hydrothermal Iron Oxide Copper-Gold and Related Deposits: A Global Perspective**. Austral Miner Fund, Adelaide, pp. 163–176.

MATHIEU, L (2018). **Quantifying Hydrothermal Alteration: A Review of Methods**. *Geosciences* 2018,8,245.

MOHSENI, S.; AFTABI, A (2015). Structural, textural, geochemical and isotopic signatures of synglaciogenic Neoproterozoic banded iron formations (BIFs) at Bafq mining district (BMD), Central Iran: The possible Ediacaran missing link of BIFs in Tethyan metallogeny. **Ore Geology Reviews**. OREGEO 1525.

MOHSENI, S.; AFTABI, A (2007). **Investigation on the Rapitan banded iron formation and mineralization in central Iranian iron ore field**: Unpublished M. Sc. thesis, Shahid Bahonar University of kerman, 284 P (in Persian).

MOKHTARI, M.A.A., Hosseinzadeh, G., Emami, M.H (2013). Genesis of iron–apatite ores in Posht-e-Badam Block (Central Iran), using REE geochemistry. **J. Earth Sci. Syst.** 122, 795–807.

MONTREUIL, J. F., CORRIVEAU, L., POTTER, E.G (2015). Formation of albititehosted uranium within IOCG systems: The Southern Breccia, Great Bear magmatic zone, Northwest Territories, Canada: **Mineralium Deposita**, v. 50, p. 293–325.

MUMIN, A.H., GOAD, R.E.; MULLIGAN, D.L (1996). **A report on the geology of the Treasure (F49508), Island 1 (F51395), Island 2 (F51396), Island 3 (F51397), and Island 4 (F49511) claims, Marian River area, Mackenzie (south) district, Northwest Territories, Canada**: NWT Geoscience Office, NORMIN Assessment Report 083776, 69 p.

NASLUND, H.R., AGUIRRE, R., DOBBS, F.M., HENRIQUEZ, F., AND NYSTRÖM, J.O (2000.). The origin, emplacement, and eruption of ore magmas: Proceedings of IX Congreso Geologico Chileno, **Actas**, v. 2, p. 135– 139.

NYSTRÖM, J.O.,HENRIQUEZ, F (1994). Magmatic features of iron ores of the Kiruna type inChile and Sweden: ore textures and magnetite geochemistry. **Econ. Geol.** 89, 820–839.

NISCO (1980). **Result of search and valuation works at magnetic anomalies of the Bafgh iron ore region during 1976- 1979**, Unpubl Rept, National Iranian Steel Corporation, 260 p.

PARAK, T(1975). Kiruna iron ores are not intrusive-magmatic ores of the Kiruna type⁶. **Econ. Geol.** 70, 1242– 1258.

PECOÏTS, E (2010). **Ediacaran iron formations and carbonates of Uruguay paleoceanographic, paleoclimatic and paleobiologic implications**. Ph.D thesis, University of Alberta, 237 p.

PERRING, C. S., POLLARD, P. J., DONG, G., NUNN, A. J., & BLAKE, K. L (2000). The Lightning Creek sill complex, Cloncurry district, northwest Queensland: A source of fluids for Fe oxide Cu-Au mineralization and sodic-calcic alteration. **Economic Geology** 95, 1067-1090.

PHILLIPS, G.N.; POWELL, R (2010). Formation of gold deposits: A metamorphic devolatilization model. **J. Metamorph. Geol.** 2010, 28, 689–718.

PILSPANEN, R., ALAPIETI, T (1977). Uralitization an example from Kuusamo, Finland . **Bull. Geol. Soc. Finland** 49, 39- 46.

POLLARD, P. J., MARK, G., & MITCHELL, L (1998). Geochemistry of post-1540 Ma granites in the Cloncurry district. **Economic Geology** 93, 1330-1344.

PORTER, T.M (2010). Current understanding of iron oxide associated-alkali altered mineralised systems: Part 1—an overview; Part 2—a review, in Porter, T.M., ed., Hydrothermal iron oxide copper-gold & related deposits: A global perspective: Adelaide, Australia, Porter **Geoscience Consultancy Publishing**, v. 3, p. 5–106.

RAMEZANI, J., TUCKER. R.D (2003). The Saghand region, Central Iran: U-Pb geochronology, petrogenesis and implications for Gondwana tectonics. **Amer. J. Sci.**, 303, 622–665.

RAMEZANI, J (1997). **Regional geology, geochronology and geochemistry of the igneous and metamorphic rock suites of the Saghand area, central Iran**: Ph.D. thesis, Washington University, St. Louis, Missouri, 416 p.

RAY, G.E., DICK, L.A (2002). The Productora deposit in north-central Chile: an example of an intrusion-related Candelaria type Fe-Cu-Au hydrothermal system. In: PORTER, T.M. (Ed.). **Hydrothermal Iron Oxide Copper-Gold and Related Deposits: A Global Perspective** PGC Publishing, Adelaide, pp. 131–151 2.

ROBB, L (2005). **Introduction to ore-forming processes**. Blackwell publishing.

ROEDDER, P.L., MACARTHUR, D., MA, X.-P., PALMER, G.R., MARIANO, A.N (1987). Cathodoluminescence and microprobe study of rare-earth elements in apatite. **Amer. Mineral.** 72, 801–811.

ROLLINSON, H. R (1993). **Using geochemical data: evaluation, presentation, interpretation**. Longman Publisher.

SABET, A., TALAB, M., ALINIA, F., GHANNADPOUR, S., HEZARKHANI, A (2015). **Geology, geochemistry, and some genetic discussion of the Chadon-Malu iron oxide-apatite deposit, Bafq District, Central Iran**. Saudi Society for Geosciences 2015.

- SADEGHÍ, B (2012). Application of fractal models to outline mineralized zones in the Zaghia iron ore deposit, Central Iran. **Journal of Geochemical Exploration** 122 (2012) 9–19.
- SAMANI, B (1993). Saghand Formation, a Riftogenic Unit of Upper Precambrian in Central Iran. **Geoscience Scientific Quarterly Journal of Geological Survey of Iran**, 2, 32-45. (In Farsi with English Abstract).
- SANGSTER, D.F (2003). The role of dense brines in the formation of vent-distal sedimentary-exhalative (SEDEX) lead-zinc deposits: Field and laboratory evidence. **Miner. Depos.** 2002, 37, 149–157.
- SILLÍTOE, R.H (2003). Iron oxide–copper–gold deposits: an Andean view. **Miner. Deposita** 38, 787–812.
- SILLÍTOE, R.H., BURROWS, D.R (2002). New field evidence bearing on the origin of the El Laco magnetite deposit, northern Chile. **Econ. Geol.** 97, 1101–1109.
- SHELLY, D (1993). **Microscopic study of Igneous and Metamorphic rock**. Champan and Hall, London, p: 184.
- SHAND, S. J (1943). **Eruptive Rocks. Their Genesis, Composition, Classification, and Their Relation to Ore-Deposits with a Chapter on Meteorite**. New York: John Wiley & Sons.
- SKIRROW, R. G (1999). Proterozoic Cu-Au-Fe mineral systems in Australia: filtering key components in exploration models. In: STANLEY, C. J. et al. (eds.). **Mineral Deposits. Processes to Processing**. Balkema, Rotterdam, 1361-1364.
- STÖCKLIN, J (1971). **Stratigraphic Lexicon of Iran**; Part 1. Geological Survey of Iran, Tehran.
- TAGHÍPOUR, S., KANANIÁN, A., SOMARÍN, A.K (2013). Mineral chemistry and alteration paragenesis of the Choghart iron oxide–apatite occurrence, Bafq district, Central Iran. **Neues Jb. Geol. Paläontol. Abh.** 269, 221–240.
- TAGHÍPOUR, S., KANANIÁN, A., MACKÍZADEH, M.A., SOMARÍN, A.K (2015). Skarn mineral assemblages in the Esfordi iron oxide–apatite deposit, Bafq district, Central Iran. **Arab. J. Geosci.** 8, 2967–2981.
- TITAYEVA, N.A (1994). **Nuclear geochemistry**, CRC Presses, p. 304.
- TRELOAR, P.J., COLLEY, H (1996). Variations in F and Cl contents in apatites from magnetiteapatite ores in northern Chile, and their ore-genetic implications. **Min. Mag.** 60, 285–301.
- TORAB, F (2008). **Geochemistry and metallogeny of magnetite- apatite deposits of the Bafq Mining District, Central Iran**. Unpublished PhD Thesis, Clausthal University of Technology, Germany.

TORAB, F.M., LEHMANN, B (2007). Magnetite-apatite deposits of the Bafq district, Central Iran: apatite geochemistry and monazite geochronology: **Min. Mag.**, v. 71, p. 347–363.

WHITNEY, PHILIP R., OLMSTED, JAMES F (1998). Rare earth element metasomatism in hydrothermal systems: The Willsboro-Lewis wollastonite ores, New York, USA, **Geochimica et Cosmochimica Acta** Volume 62, Issue 17, September 1998, Pages 2965–2977.

WILLIAMS, P.J., BARTON, M.D., FONTBOTÉ, L., DE HALLER, A., JOHNSON, D.A., MARK, G., MARSCHIK, R., OLIVER, N.H.S (2005). Iron-oxide–copper–gold deposits: geology, space–time distribution, and possible modes of origin. **Economic Geology**, pp. 371–406 (100th Anniversary Volume).

WYBORN, L. A. I (1998). Younger ca. 1500 Ma granites of the Williams and Naraku batholiths, Cloncurry district, eastern Mt Isa Inlier: geochemistry, origin, metallogenic significance and exploration indicators. **Australian Journal of Earth Sciences** 45, 397-411.

ACKNOWLEDGEMENTS

The present study is based on the first author's PhD thesis at Science and Research branch of the Islamic Azad University, Tehran, Iran. The authors would like to thank the editor and referees for their critiques and suggestions that helped to improve the quality of the paper. This work was supported by the Iran Minerals Production & Supply Co. (IMPASCO) and IMIDRO. The authors express their gratitude to the managers of the ICIOC (Iranian Central Iron Ore Co.).